Electronic structure of a σ-FeCr compound

2008 J. Phys.: Condens. Matter 20 235234

(http://iopscience.iop.org/0953-8984/20/23/235234)

J. Phys.: Condens. Matter **20** (2008) 235234 (6pp) doi:10.1088/0953-8984/20/23/235234

Electronic structure of a σ-FeCr compound

J Cieslak[1,3], J Tobola[1], S M Dubiel[1], S Kaprzyk[1], W Steiner[2] and M Reissner[2]

[1] Faculty of Physics and Applied Computer Science, AGH University of Science and Technology, al. Mickiewicza 30, 30-059 Krakow, Poland
[2] Institute of Solid State Physics, Vienna University of Technology, A-1040 Wien, Austria

E-mail: cieslak@novell.ftj.agh.edu.pl

Received 28 January 2008, in final form 2 April 2008
Published 9 May 2008
Online at stacks.iop.org/JPhysCM/20/235234

Abstract

The electronic structure of a σ-FeCr compound in a paramagnetic state was calculated for the first time in terms of isomer shifts and quadrupole splittings. The former were calculated using the charge self-consistent Korringa–Kohn–Rostoker (KKR) Green's function technique, while the latter were estimated from an extended point charge model. The calculated quantities combined with recently measured site occupancies were successfully used to analyze a Mössbauer spectrum recorded at room temperature using only five fitting parameters namely background, total intensity, linewidth, IS0 (necessary to adjust the refined spectrum to the used Mössbauer source) and the QS proportionality factor. Theoretically determined changes of the isomer shift for the σ-FeCr sample were found to be in line with the corresponding ones measured on a α-FeCr sample.

(Some figures in this article are in colour only in the electronic version)

1. Introduction

The σ-phase belongs to the so-called Frank–Kasper phases, whose characteristic feature is a complex crystallographic structure, and, in particular, high coordination numbers. Consequently, understanding of the physical properties of such phases has been not straightforward and easy. In particular, the time that elapsed between its discovery [1] and the identification of its crystallographic structure [2] was about 30 years. The complexity of the structure results in difficulties both in the interpretation of the experimental results as well as in the theoretical calculations. Concerning the latter, only a few papers have been published on the σ-phase in the Fe–Cr system, none of them related to its electronic structure. Nowadays, over 50 examples of binary alloy systems are known in which the σ-phase is formed [3]. It occurs often in materials that are technologically important and its presence drastically deteriorates their mechanical properties. Hence, the basic investigation of structural, electronic and magnetic properties is of quite general interest.

The Fe–Cr σ-phase precipitates from the α-phase during an isothermal annealing in the temperature range of $\sim$530 °C $< T <$ $\sim$830 °C mostly on the grain boundaries and in the form of sub-micrometer sized needles and/or lamellae. Its physical properties are substantially different from those characteristic of the α-phase (bcc), from which it precipitates [3].

Mössbauer spectroscopy belongs to the most suitable methods for the investigation of the structural properties and magnetic behavior of the Fe–Cr σ-phase. This stems from its high sensitivity to the hyperfine parameters, which are strongly influenced by the local configuration of nearest neighbor (NN) atoms of the ^{57}Fe atom probe. A typical Mössbauer spectrum of the Fe–Cr σ-phase must be composed of at least five subspectra with various intensities related to the iron occupation of five inequivalent crystallographic sites. Although the corresponding hyperfine parameters (isomer shift, IS and quadrupole splitting, QS) differ from each other, the differences are comparable or smaller than the typical experimental linewidths. Consequently, the spectrum is not well resolved, even below the Curie temperature ($T_c \sim$ 30 K in σ-$Fe_{53.8}Cr_{46.2}$). Some of the parameters describing the spectrum could be determined in other experiments

[3] Author to whom any correspondence should be addressed.

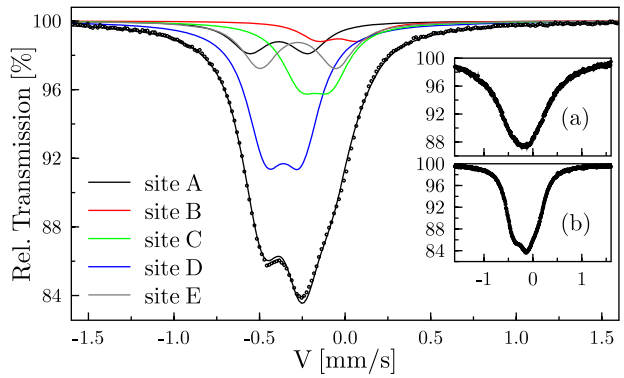

Figure 1. ^{57}Fe Mössbauer spectrum of the σ-$Fe_{53.8}Cr_{46.2}$ alloy recorded at 300 K (dots) compared to the calculated one (solid line). The subspectra related to the inequivalent sites are indicated by colored lines. The spectra recorded at (a) 4.5 K and (b) 35 K are shown in the insets for comparison.

(e.g. relative subspectra contributions should be proportional to the Fe concentrations on particular sites determined in the neutron diffraction experiment), but the rest (IS, QS and linewidths Γ) should be obtained from the fitting procedure. Unfortunately, the number of known parameters is too small and decomposition of the overall spectrum is not a unique task, since one can make several mathematically correct fits with different sets of fitting parameters. For that reason we decided to calculate the electronic structure and the resulting hyperfine parameters (IS, QS), in various atomic configurations of the σ Fe–Cr system in order to interpret the experimental Mössbauer spectrum.

The earlier electronic structure computations of the transition-element σ-phase focused mainly on crystal stability and site occupancy preference of the constituent atoms on five inequivalent sites [4]. Later, it was reported [5] from the full potential linearized augmented plane waves (FLAPW) method that the calculated formation energy in Fe–Cr and Co–Cr σ-phases remained in reasonable agreement with measured enthalpies. Finally, the vibrational properties of the Fe–Cr σ-phase were investigated by means of molecular dynamics simulation [6], which showed some similarities to vibrational behaviors of the glassy state.

The aim of our work is to calculate the electronic structure and resulting hyperfine parameters for the most plausible atomic configurations of the σ-FeCr system in order to reconstruct the experimental Mössbauer spectrum in the paramagnetic state.

2. Experimental details

The procedure of σ-$Fe_{53.8}Cr_{46.2}$ sample preparation is given in detail elsewhere [7]. ^{57}Fe Mössbauer spectra were recorded in transmission geometry using a standard spectrometer and a ^{57}Co/Rh source for the 14.4 keV gamma rays at temperatures 4.5, 35 and 300 K. They are presented in figure 1. At first glance, one notices that the spectra measured above the Curie temperature (35 and 300 K) are quite similar, whereas a small magnetic splitting can be observed at 4.5 K. In this work we focus on the paramagnetic state only.

Table 1. Atomic crystallographic positions and numbers of NN atoms for the five lattice sites of the Fe–Cr σ-phase.

Site	Crystallographic positions	NN					
		A	B	C	D	E	Total
A	2i (0, 0, 0)	—	4	—	4	4	12
B	4f (0.4, 0.4, 0)	2	1	2	4	6	15
C	8i (0.74, 0.66, 0)	—	1	5	4	4	14
D	8i (0.464, 0.131, 0)	1	2	4	1	4	12
E	8j (0.183, 0.183, 0.252)	1	3	4	4	2	14

3. Computational details

The charge and spin self-consistent Korringa–Kohn–Rostoker Green's function method [8, 9, 11] was used to calculate the electronic structure of the Fe–Cr σ-phase. The crystal potential of muffin-tin (MT) form was constructed within the local density approximation (LDA) framework using the Barth–Hedin formula [10] for the exchange–correlation part. The group symmetry of the unit cell of the σ-phase ($P4_2/mnm$, #136) was lowered to allow for various configurations of Fe/Cr atoms. The experimental values of lattice constants [7] ($a = 8.7891$ Å, $c = 4.5559$ Å) and atomic positions (table 1) were applied in all computations. For fully converged crystal potentials electronic density of states (DOS), total, site-composed and l-decomposed DOS (with $l_{max} = 2$ for Fe and Cr atoms) were derived. Fully converged results were obtained for ∼120 special **k**-point grids in the irreducible part of the Brillouin zone but they were also checked for convergence using a more dense **k**-mesh. Electronic DOSs were computed using the tetrahedron **k**-space integration technique and ∼700 small tetrahedra [12].

3.1. Structural aspects

As aforementioned, the σ-phase has a complex close-packed tetragonal structure with 30 atoms in the unit cell. Atoms are distributed over five nonequivalent sites, called A, B, C, D and E, the population of them is shown in table 1. Each position can be characterized by:

(i) the total number of nearest neighbors (NN),
(ii) their belonging to one of five sublattices,
(iii) the distances to NN atoms,
(iv) the occupancy by Fe or Cr atoms.

The former three properties (i–iii) can be derived directly from the space group information and are presented in tables 1 and 2. Each atom in the σ-phase structure is surrounded by 12–15 atoms belonging to various sites (all NN configurations except for A–A and A–C are possible). Their interatomic distances range from 2.265 Å (E–E) to 2.922 Å (B–E) (see table 2 for average values) and can be slightly different even within the same pairs of atoms (e.g. for C–D three different values can be noticed). Moreover, the NN spatial distribution is not far from spherical for each site. Site-occupation parameters as found from the neutron diffraction data [7] are presented in table 3. It clearly shows that all five sites are populated by both alloy constituting elements. The distribution of Fe and

Table 2. Distances between NN atoms for five lattice sites of the Fe–Cr σ-phase. The average values with standard deviations (in parentheses) are indicated, when more than one distance is possible. The corresponding weighted mean values (d_{av}) are given in the last row.

	Distances (Å)				
Site	A	B	C	D	E
A	—	2.605	—	2.366	2.547
B	2.605	2.519	2.420	2.695	2.864(0.005)
C	—	2.420	2.749(0.196)	2.487(0.004)	2.766(0.006)
D	2.366	2.695	2.487(0.004)	2.422	2.549(0.019)
E	2.547	2.864	2.766(0.006)	2.549(0.019)	2.280(0.018)
d_{av}	2.506	2.702	2.655	2.572	2.640

Table 3. Fe site-occupation parameters of the σ-FeCr alloy, experimental and assumed for calculations. N_t stands for the percentage of the total Fe atoms in the site (referred to the 30 atom unit cell), whereas N describes the number of Fe atoms occupying the site. N_{cal} represents the value used in the KKR calculations. The corresponding relative occupancy (percentage) is given in parentheses. The quadrupole splitting values QS for five lattice sites as obtained from the fitting procedure are presented in the last column.

Site	N_t	N	N_{cal}	QS (mm s^{-1})
A	11.3	1.826 (91.3)	2 (100.0)	0.34
B	6.4	1.040 (26.0)	1 (25.0)	0.24
C	20.5	3.304 (41.3)	3 (37.5)	0.18
D	44.9	7.208 (90.1)	7 (87.5)	0.21
E	17.0	2.744 (34.3)	3 (37.5)	0.45

Cr atoms over these sites is neither random nor fully ordered, but within each of the five crystallographic positions it remains random [7]. The electronic structure and hyperfine interactions of such complex and disordered systems might be investigated by the well-established coherent potential approximation (CPA) combined with the KKR method [11]. However, the KKR-CPA computations of the binary σ-phase are (at the moment) too complicated and highly time-consuming to obtain acceptable results in a reasonable time. Additionally, the CPA approach tends to average the parameters over all possible Fe/Cr configurations for the given lattice site. On the other hand, hyperfine interactions, which are the subject of the Mössbauer investigations, are mainly sensitive to the local NN-configuration changes. For that reason we lowered the symmetry of the unit cell (space group $P4_2/mnm$) to the simple tetragonal one, and the calculations were carried out for defined atom configurations using the KKR method adapted to ordered systems. In practice, the tetragonal unit cell and atomic positions were unchanged but variable occupancy made all 30 atomic positions crystallographically nonequivalent. In such a specified unit cell each of the crystallographic positions was occupied exclusively either by Fe or Cr atom. However, in our numerical attempts we were constrained by the experimental Fe/Cr concentrations on each of the five lattice sites and the considered composition should be as close as possible to the measured stoichiometry of the σ-$Fe_{53.8}Cr_{46.2}$. The concentrations used are given in table 3. For example, the experimentally observed Fe occupancy of site C (8i) was found to be $P(\mathrm{Fe, C}) = 0.413$, whereas in our computations, having eight atoms on the position previously defined as 'C', we had to assume five Cr and three Fe atoms to reach the closest concentration. It is worth noting that each lattice site is surrounded by all other crystallographic sites occupied by either Fe or Cr, which can be distributed in different ways. For the above-mentioned example of the C site, one can distinguish 56 possible nonequivalent Fe–Cr arrangements and over 10^5 possibilities for all 30 atoms in the unit cell. Fortunately, there is no need to analyze all possible arrangements because their influence on the hyperfine parameters can be accounted for by the number of Fe/Cr atoms in the nearest shell of the specified ^{57}Fe atom. Consequently, it was enough to restrict our calculations to arbitrarily chosen atom configurations (26 different arrangements), which covered most of all the possible NN-values for each of the five lattice sites. Indeed, the above-mentioned assumptions were later supported by almost linear correlations between calculated charge densities at the Fe nucleus and its Fe-NN numbers for all five lattice sites, separately. These correlations were used in further calculations.

3.2. Isomer shift, IS

The isomer shift is proportional to the difference between the electron densities in the range of the nucleus for source and absorber atoms:

$$\mathrm{IS} = \frac{2\pi}{5} Z S(Z) e^2 R^2 \frac{\Delta R}{R} [\rho_A(0) - \rho_S(0)] \qquad (1)$$

where Z is the nuclear charge of the Mössbauer absorber, $S(Z)$ is a relativistic correction factor, e is the elementary charge, R is the average radius of the Mössbauer nucleus in the ground and excited state and the ΔR is the difference of these two radii. $\rho_i(0)$ is the non-relativistic electron density at the nucleus for the Mössbauer absorber ($i = A$) or source ($i = S$), which is in practice derived from extrapolation of the electron charge density to $r = 0$. Since all factors except the electron density of the absorber are constant for a given spectrum, it is sufficient for our purpose to consider a simplified equation for the IS as follows:

$$\mathrm{IS} = a[\rho_A(0) - b] \qquad (2)$$

with a and b constants as determined in the calibration procedure. According to [13], the value of a may vary from 0.367 to 0.403 (au^3 mm s^{-1}) (au being atomic units). In our work the average value of $a = 0.385$ (au^3 mm s^{-1}) was used. Since only differences between isomer shifts for particular subspectra are important in the fitting procedure, the b-value was assumed to be equal to 0.

3.3. Quadrupole splitting, QS

The shifts in the energy levels resulting from the interaction between the nucleus with a quadrupole moment eQ and the electric field gradient (EFG) are obtained from

$$\Delta E = \frac{eQV_{zz}}{4I(2I-1)} [3m^2 - I(I+1)](1 + \eta^2/3)^{1/2} \qquad (3)$$

where $V_{zz} = \partial^2 V/\partial z^2$ is the largest component of EFG along a principal axis and $\eta = (V_{xx} - V_{yy})/V_{zz}$ is the asymmetry parameter. The source of EFG at the nucleus is the character of the surrounding electron charge distribution. There are two principal classifications of this external charge:

(a) the electrons directly associated with the Fe nucleus, the so-called valence contribution V_{zz}^{val},
(b) the charges of other atoms in the lattice, the so-called lattice contribution V_{zz}^{lat}.

Hence, the EFG tensor depends on both components [14].

In the most widely used computational approach, charges external to the central atom are treated as point charges. Hence, the V_{ij}-values can be easily calculated according to the formula

$$V_{ij} = \sum e_i (3x_i x_j - r^2 \delta_{ij}) r^{-5} \tag{4}$$

where $x_1 = x$, $x_2 = y$, $x_3 = z$, e_i is the electronic charge on neighboring atom i and δ_{ij} denotes the Kronecker symbol. In this work the procedure for deriving the EFG tensor was extended to the electron density distributed around each atom, which goes beyond the point charge approximation. In practice, the electron cloud inside each MT sphere was divided into over 10^5 small volume elements, which represented point charges in equation (4). Radial charge density distributions for Fe ($\rho_i^{\mathrm{Fe}}(r)$) and Cr ($\rho_i^{\mathrm{Cr}}(r)$), where i denotes each of 30 atoms in the unit cell, were obtained from the KKR calculations for each atom and for all considered atom configurations. In the next step, the mean radial charge density distributions were calculated using an averaging procedure, i.e. for each of five lattice sites the $\rho_L(r)$ (with L = A through E) was computed by averaging earlier calculated charge density distributions weighted by the effective occupancy of Fe/Cr on each site. Using these $\rho_L(r)$ dependences, V_{ij} was evaluated (equation (4)) by summation in the variable distance (in each crystallographic direction) from the fixed atom. The procedure was carried out with increasing summation distance until resulting EFG-values became stable (the difference less than 0.1%). Finally, satisfactory results were obtained for a cube of seven lattice constants around the ^{57}Fe atom, containing 3375 nearest unit cells (over 10^5 atoms and electron densities inside their MT spheres). The resulting EFG-tensors were then used to calculate the energy shift values ΔE for each lattice site.

The interaction between V_{zz}^{lat} and the quadrupole moment of the ^{57}Fe-nucleus is complicated by the presence of the Mössbauer atom's own electrons, especially in d-states. On the other hand, since the charge density distribution around each atom in the MT approximation is spherically symmetric, the calculated V_{zz}-value related to the valence electron's cloud vanishes, which is a serious limitation of this approach. For that reason we have to assume that the influence of V_{zz}^{lat} is dominant and V_{zz}^{val} is proportional to V_{zz}^{lat}. Consequently, the calculated energy shift values ΔE are proportional to the QS-values. The proportionality factor γ was assumed to be identical for all lattice sites, and was calculated in the fitting procedure of the experimental data. The resulting QS-values are shown in table 3. It must be mentioned that the obtained QS-values are only average values for each lattice site.

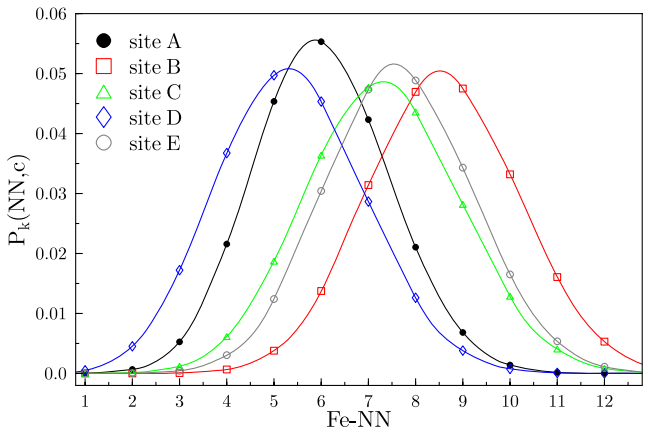

Figure 2. Probability $P_k(\mathrm{NN}, c)$ for finding NN-Fe atoms in the first coordination shell for the five inequivalent lattice sites in σ-$Fe_{53.8}Cr_{46.2}$. $k = A \cdots E$, see equation (6). The solid lines are shown as a guide for the eye only.

4. Results and discussion

4.1. Probability distribution calculation

Since hyperfine parameters depend mainly on the NN configuration, it is worth calculating the probability of finding a definite number of Fe atoms in the nearest shell for each lattice site. In the case of a random distribution one can use the Bernoulli formula describing the probability of finding n atoms of type X in $X_c Y_{1-c}$ alloy

$$P_{\mathrm{B}}(n, c) = \binom{N_{\mathrm{tot}}}{n} c^n (1-c)^{N_{\mathrm{tot}}-n} \tag{5}$$

where N_{tot} stands for the total number of NN atoms and c is the atomic concentration of X. In the case of the σ-phase there are five different NN-types with different N_{tot} and c values on each site. The NN atoms are distributed on the specified lattice sites (table 1), so the formula for the kth site should be modified:

$$P_k(\mathrm{NN}, c) = \sum \prod_{i=1}^{5} P_{\mathrm{B}}(\mathrm{NN}_i, c_i); \qquad \mathrm{NN} = \sum_{i=1}^{5} \mathrm{NN}_i \tag{6}$$

where index i denotes the crystallographic site, the summation in equation (6) runs over all possible combinations of NN_i yielding NN, and c is the atomic concentration of Fe. This procedure allows us to calculate the probability distribution for each site separately. As can be clearly seen in figure 2, all distributions are Gaussian-like curves with similar linewidths but shifted relative to each other. The most probable numbers of Fe-NN atoms are markedly different for each site and vary from 5 (D site) to 9 (B site).

4.2. Charge density distributions

The electron densities at the nucleus for the Mössbauer absorber $\rho_A(0)$ were calculated for each lattice site of the Fe–Cr σ-phase. Figure 3 summarizes our results, depicting the dependences of $\rho_A(0)$ on the number of Fe-NN atoms. One can notice correlations between these quantities, which agree

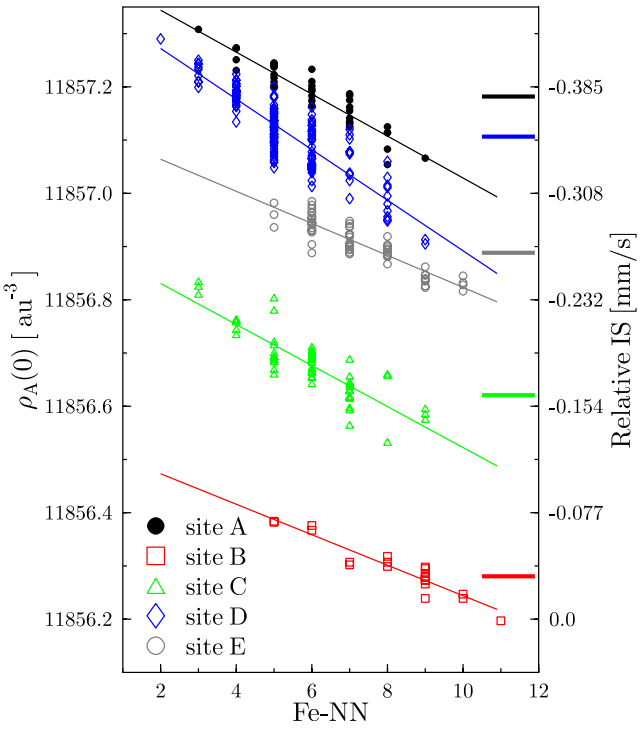

Figure 3. Electron densities at the nucleus of Fe calculated for each lattice site of the Fe–Cr σ-phase (left scale) or, equivalently, isomer shifts relative to the source, IS (right scale). Solid lines represent the best linear fits between the ρ_A values and the number of Fe-NN atoms. Different symbols denote the calculated ρ_A values corresponding to inequivalent sites. The average values of the charge density (or isomer shifts relative to the source, IS_{av}) are indicated on the right-hand side of the graph.

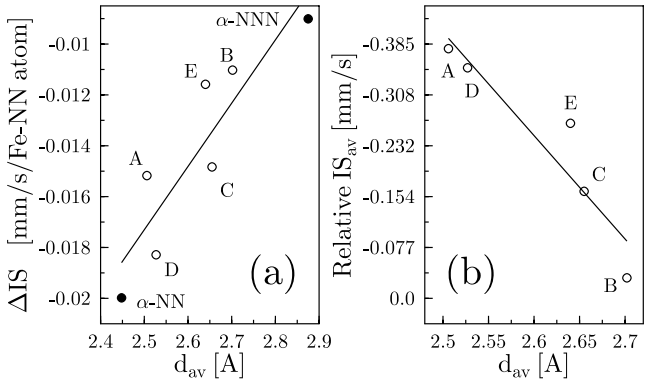

Figure 4. (a) The slope of the isomer shift, ΔIS, dependence versus average NN distance, d_{av}. Empty and filled circles stand for the Fe–Cr σ- and α-phase, respectively. (b) The relative to the source average isomer shift IS_{av} versus d_{av}.

well with the anticipated relations. The slopes of the linear regressions are quite similar and negative (-0.04 au^{-3} per one Fe-atom in the first coordination shell on average) for all sites, which means that one Fe-NN atom decreases the isomer shift value by $\Delta IS \sim 0.013$ mm s^{-1}. The particular slopes calculated for the σ-phase can be compared to two experimentally obtained values for the Fe–Cr α-phase. In this case, ΔIS equal to 0.020 mm s^{-1} and 0.009 mm s^{-1} for the first and the second neighbor shell, respectively, when one Fe-neighbor atom is added [15, 16]. A correlation between ΔIS for the Fe–Cr α- and σ-phases and the average interatomic distances d_{av} is presented in figure 4(a). We see that these quantities markedly decrease in absolute value with increasing distance, as can be expected. Also the average isomer shift relative to the source IS_{av} decreases monotonically with d_{av}-values and becomes the lowest for the closest neighbors (site A), as shown in figure 4(b). The determined IS_{av} remain significantly different for each crystallographic position.

4.3. RT Mössbauer spectrum analysis

In our analysis we reasonably assumed the Mössbauer spectrum to be composed of five subspectra, each of them represents the distribution of the IS. The relative area under each subspectrum corresponding to the particular site should be equal to the number of Fe atoms occupying this site. The differences between the Lamb–Mössbauer factors for nonequivalent positions were considered to be very small, thus these factors were identical in our analysis. Also, the Γ-values were assumed to be the same for all lines.

The RT Mössbauer spectrum was successfully fitted using the least square method. The relative subspectra intensities were assumed to be known from recent neutron diffraction experiments [7], whereas QS- and IS-values relative to the source as well as the distinct linear dependence of IS on the NN-Fe atoms were obtained from our KKR calculations. Each subspectrum was constructed as a sum of double lines with the same QS-values, IS-values linearly dependent on Fe-NN numbers and probabilities determined according to equation (6). It should be mentioned here that there are only five fitting parameters in the model, namely: background, total intensity, isomer shift for the B site subspectrum IS0 (necessary to adjust the refined spectrum to the used Mössbauer source), linewidth Γ and proportionality factor γ. The background, total intensity and IS0 depend on the measurement conditions only, whereas the two latter parameters are directly connected with the intrinsic properties of the Fe–Cr σ-phase.

5. Conclusions

In summary, we have calculated the electronic structure in terms of the hyperfine parameters such as the isomer shift and the quadrupole splitting of the σ-phase in the FeCr system. Theoretically calculated values of the spectral parameters were successfully used in combination with experimentally determined site-occupation probabilities to fully reconstruct a ^{57}Fe site Mössbauer spectrum recorded at room temperature on the σ-FeCr sample, using only five adjustable parameters (background, total intensity, Γ, IS0 and γ factor). It was also shown that theoretically determined ΔIS-values and average IS-values remain in line with the corresponding quantities measured in the α-FeCr phase. The latter means that in both phases the Fe site charge density scales linearly with NN and NNN distances. Similar scaling behavior of the charge density (isomer shift) has been shown to exist for the number of NN-Fe atoms. It is, however, characteristic of a given site.

Acknowledgments

This work was partly supported by the Polish Ministry of Science and Higher Education and ÖAD Project 20/2003 as well as grant No. N202210433.

References

[1] Bain E C 1923 *Chem. Met. Eng.* **28** 23
[2] Bergman G and Shoemaker D P 1954 *Acta Crystallogr.* **7** 857
[3] Hall E D and Algie S H 1966 *Metall. Rev.* **11** 61
[4] Sluiter M, Esfariani K and Kawazoe Y 1995 *Phys. Rev. Lett.* **75** 3142
[5] Havrankova J, Vřeštal J, Wang L G and Šob M 2001 *Phys. Rev.* B **63** 174104
[6] Simdyankin S I, Taraskin S N, Dzugutov M and Elliott S R 2000 *Phys. Rev.* B **62** 3223
[7] Cieslak J, Reissner M, Dubiel S M, Wernisch J and Steiner W 2008 *J. Alloys Compounds* at press doi:10.1016/j.jallcom.2007.05.098
[8] Butler W H, Dederichs P, Gonis A and Weaver R (ed) 1992 *Applications of Multiple Scattering Theory to Materials Science* (*MRS Symposia Proceedings* vol 253) (Pittsburgh, PA: MRS) chapter III
[9] Stopa T, Kaprzyk S and Tobola J 2004 *J. Phys.: Condens. Matter* **16** 4921
[10] Barth U von and Hedin L 1972 *J. Phys. C: Solid State Phys.* **5** 1629
[11] Bansil A, Kaprzyk S, Mijnarends P E and Tobola J 1999 *Phys. Rev.* B **60** 13396
[12] Kaprzyk S and Mijnarends P E 1986 *J. Phys. C: Solid State Phys.* **19** 1283
[13] Neese F 2002 *Inorg. Chim. Acta* **337** 181
[14] May Leopold (ed) 1971 *An Introduction to Mössbauer Spectroscopy* (New York: Plenum)
[15] Dubiel S M and Inden G 1987 *Z. Metallk.* **78** 544
[16] Dubiel S M and Zukrowski J 1981 *J. Magn. Magn. Mater.* **23** 214